Few-cycle mid-infrared pulse full characterization in single shot

Canhua Xu (许灿华), Chuang Li (李 闯), Liwei Song (宋立伟), Ding Wang (王 丁), and Yuxin Leng (冷雨欣)*

State Key Laboratory of High Field Laser Physics, Shanghai Institute of Optics and Fine Mechanics, Chinese Academy of Sciences, Shanghai 201800, China

**Corresponding author: lengyuxin@siom.ac.cn*

Received April 20, 2012; accepted June 20, 2012; posted online October 24, 2012

We build a frequency resolved optical gating (FROG) setup based on the second harmonic generation (SHG) FROG to characterize the mid-infrared (MIR) few-cycle laser pulse in single shot basis. Considering the extremely wide bandwidth, we use 20-μm-thick BBO crystal as the nonlinear medium, and correct the spectral response with the frequency summing efficiency. Spatial splitting is adopted to avoid additional material dispersion. In combination with a 4f imaging, this configuration enables the setup to run in single shot. With the central wavelength of 1.8 μm, the measured pulse has a duration of 9.3 fs, which corresponds to about 1.5 cycles.

OCIS codes: 320.7090, 320.7100, 320.7160, 140.7090.
doi: 10.3788/COL201210.123202.

In recent years, high harmonic generation (HHG) and attosecond pulse driven by intense short-pulse laser are initiating a revolution in measurement[1,2] and control of ultrafast electron dynamics in various matter[3−5]. So far the shortest 80 as isolated pulse is driven by high intensity few-cycle 0.8-μm Ti:sapphire laser[6]. Theory and experiments indicate that the longer wavelength of the driving laser is in favor of producing higher order harmonics and shorter attosecond pulses[7].

Several milli-Joule ultrafast laser systems with the wavelength ranged from 1.5 to 3 μm were demonstrated over the past few years[8−10]. In general, several tens femtosecond pulses at 0.8-μm wavelength from a Ti:sapphire laser system are amplified and frequency-shifted to mid-infrared (MIR) range by optical parametric amplification (OPA) or optical parametric chirped-pulse amplification (OPCPA). Typically high intensity and few-cycle duration are realized by spectrum broadening in a gas-filled hollow-core fiber (HCF) or a filament, followed by spectral phase compensation using chirped mirrors or anomalous dispersion materials[9]. In the few-cycle regime, the light-matter interaction is extremely sensitive to the pulse shape and spectral phase. Therefore a full characterization of both amplitude and phase is crucial for the pulse compression and HHG experiments.

Ultrafast pulse full characterization technologies mainly include spectral phase interferometry for direct electric field reconstruction[11] (SPIDER) and frequency -resolved optical gating[12,13] (FROG). After proper considering various spectrum and temporal weighting factors, FROG was successfully used to characterize the 0.8-μm Ti:sapphire ultrafast pulse with duration of 4.5 fs in 1998[14]. Subsequent reports illustrated FROG measurements were available for various wavelengths[15,16] and pulse lengths[17]. In 2008 a single-shot FROG with a compact geometry was demonstrated to measure the 1.5-cycles pulse in the near infrared (NIR) range[18]. Combining with the improved rapid retrieve algorithm, the single-shot measurement is very helpful for online monitoring and optimization of the chirp compensation, which is even more important for the low frequency high energy amplification system.

In this letter, we present a single-shot FROG setup to characterize a 1.8 μm-centered few-cycle pulse generated by a home-built OPA system. The single-shot measurement was realized by the nonlinear second harmonic (SH) arrangement in a thin BBO crystal and precise imaging a charged-coupled device (CCD) camera. A 20° cut-angle BBO crystal with 20-μm thickness and a low density grating were applied to adapt the particular and ultra-broad spectrum. With the center-wavelength of 1.8 μm, the pulse duration was characterized to be 9.3 fs, which corresponded to about 1.5 optical cycles in this regime.

The high intensity MIR ultrafast system was described in Ref. [9]. Briefly, the measured pulses with the wavelength tunable from 1.2 to 2.4 μm are generated by a BBO-based three-stage OPA system driven by an 8-mJ, 1-kHz, 57-fs Ti:sapphire laser (Coherent LEGEND-Cryo). The maximum energy of single pulse reaches 1.6 mJ with the center wavelength of 1.8 μm. The spectrum of amplified pulse is stretched in a 1-m-long Ar-filled HCF and compensated by a 2-mm fused silica material with anomalous dispersion in MIR range. As a result, 0.7-mJ pulse energy is compressed into near limit of Fourier transform to few cycle.

Figure 1 shows the setup for the full characterization of the aforementioned pulse both in amplitude and phase. The measured pulse is split spatially into two semicircular sub-beams by two D-shape reflective plane mirrors, which are separately mounted on the top of each other. The two sub-beams propagate with a small crossing angle about 3° in the horizontal plane, and meet each other on the front surface of a 20-μm BBO crystal with the cut-angle of 20°. The following lens is used to image the front surface of crystal to CCD camera in a 4f geometry. This arrangement directly presents the delays of two sub-beams as various positions in one direction on the CCD, and makes single-shot measurement possible.

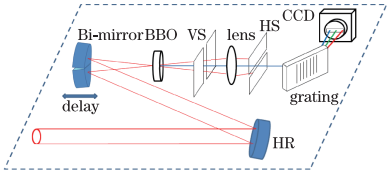

Fig. 1. Sketch of single-shot SHG-FROG for measurement of MIR pulse in near single cycle regime. Bi-mirror consists of two D-shape flat mirrors, which can split input pulse into two sub-beams in horizontal direction.

A line-shape center part of the beam is filtered out by a vertical slit (VS) mounted as close as possible to the BBO crystal. Due to the maximum separation of the fundamental and SH spots in the focal distance of the lens (7.5 cm), a horizontal slit (HS) is used to block the fundamental beam. The width of the slit is about 0.5 mm, which is a trade-off between detectable intensity and the clarity of diffraction patterns of the grating. A low density grating with 300-line per millimeter is mounted in an appropriate position to fit the extremely broad spectrum and limited aperture size of the CCD camera. The entire setup can be confined in a 20×20 (cm) area in a compact design.

The calibration of the FROG setup, i.e, the measured FROG trace, includes two dimensions: delay and spectrum. The delay interval corresponding to every pixel in the trace can be determined by moving one of the semicircular mirrors back and forward to manually induce the delay of two sub-beams, and observe the center shifting of the trace in CCD camera[19]. Linear dependence of the center shifting to mirror displacement gives 1.23-fs per pixel in FROG trace. Usually the calibration of the spectrum is performed with broadband halogen lamps. With the absence of the lamps, the calibration can also be carried out by comparing the frequency marginal (integral along the delay dimension) with the spectrum convolution of the fundamental pules. Theoretically these two curves should be identical if the spectrum response of the setup is uniform[19], according to

$$M(2\omega) = \int M(\xi)M(\omega-\xi)\mathrm{d}\xi = \int I_{\mathrm{FROG}}(\omega,\tau)\mathrm{d}\tau, \quad (1)$$

where $M(\omega)$ and $M(2\omega)$ are the spectral intensities of fundamental and SH pulses, respectively; ω is the frequency; τ is the delay between two sub-beams. In order to avoid the error induced by the spectrum stretching in the Ar-filled HCF, we recorded the spectrum of the OPA pulse passing through the vaccum HCF with a fiber spectrometer (NIR 256, Ocean Optics). The calculated convolution of this spectrum and the marginal integral of the corresponding FROG trace are in good agreement with each other as Gaussian-like curves. The comparison of the full-width at half-maximum (FWHM) of two curves yielded a 0.24-nm spectral interval for every pixel in spectral axis. And we kept the setup unchanged and only increased the gas pressure in subsequent few-cycle pulse measurements.

The inhomogeneity of the spectral response in a SHG-FROG setup mainly derives from the various efficiencies during frequency summing process. Figure 2 shows the dependence of the SH efficiency to the wavelength in BBO crystals with the same cutting angle and different thicknesses[20]. Apparently, the SH bandwidths of the 10- and 20-μm BBO crystals are abundant for the few-cycle pulse with the spectrum ranged from 1.2 to 2.4 μm, which the thicker crystal has weak and irregular weighting at the long wavelength. One interesting point is that in MIR range, it has more relaxed restrictions in terms of crystal thickness compared with 5-μm BBO used for few-cycle 0.8-μm Ti:sapphire pulse[19]. In our setup, a 20-μm BBO was used. Therefore for the spectral response correction, we divided the measured FROG traces by the solid curve in Fig. 2 along the spectrum direction before using the retrieve algorithm. Although the grating diffraction efficiency and CCD detector sensitivity may also induce inhomogeneous spectral response, due to the limitation of experimental condition, we did not implement other additional calibrations in this work.

The measured and retrieved FROG traces after correction are plotted in Figs. 3(a) and (b), respectively. Several reasons including wave-front phase distortion[21], the spectrum broadening process in HCF or improper alignment of the setup may be responsible for the asymmetric structure in the trace. It greatly slows down the convergence of the retrieve algorithm and needs to be eliminated as much as possible. The principal component generalized projections algorithm[22] (PCGPA) was used to retrieve the amplitude and phase of the pulse. The FROG error[20] in a 256×256 matrix used in retrieving program can be calculated by

$$\mathrm{ERROR} = \left\{\frac{1}{N^2}\sum_{\omega,\tau=1}^{N}[I_{\mathrm{measured}}(\omega,\tau) - |E_{\mathrm{retrieved}}(\omega,\tau)|^2]^2\right\}^{1/2}, \quad (2)$$

where N=256, I is the measured trace intensity, and E is the amplitude of retrieved electric field.

The retrieved result is given by minimizing the difference between the measured and calculated FROG traces, the slight asymmetry remains in the retrieved traces. Considering the above-mentioned experimental imperfection, theoretically if the two sub-beams in retrieving slightly differ, the retrieved trace will be asymmetric in delay direction even in a SHG-FROG setup. A small error of 0.007 confirms the convergence of the algorithm and the validity of our setup. Figures 3(c) and (d) show the retrieved intensity and phase in temporal domain and spectral domain respectively. In Fig. 3(d) the multi-peaks is a well-resolved feature of the

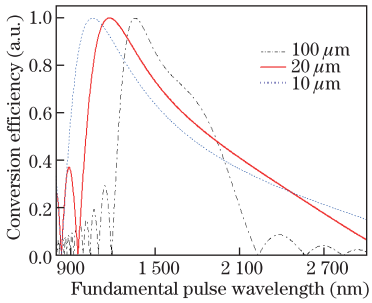

Fig. 2. SH efficiency of FROG setup with different thickness BBO crystals. When the measured pulses duration is down to near-single-cycle in MIR regime, the thickness of BBO crystal is limited in 20 μm.

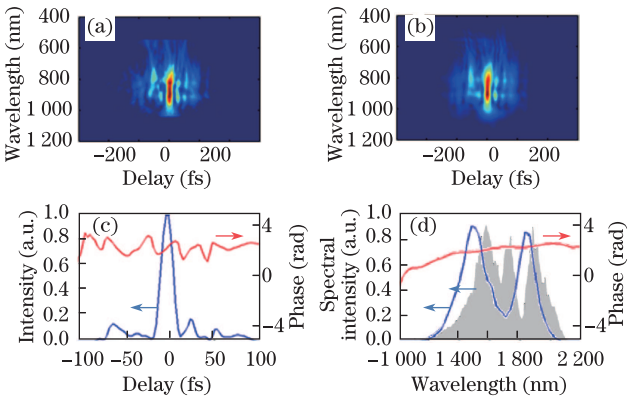

Fig. 3. (a) Measured FROG trace; (b) retrieved FROG trace. FROG error is 0.007 for 256×256 matrix used in retrieve algorithm. (c) Retrieved pulse intensity and phase in temporal domain shows that the duration is 9.3 fs. (d) Retrieved intensity and phase in spectral domain. The experimental spectrum (shaded) supports 9.0 fs pulse of Fourier transform limitation. It means that the detected pulse has a very small TBP of 1.03.

stretched spectrum in the gas-filled HCF. The experimental spectrum of the fundamental pulse is shown as a shaded area. The discrepancy between the measured and retrieved spectra contributes to the different responses of grating and CCD camera at the various wavelengths, which is not corrected in this letter. A theoretical Fourier transform of the experimental spectrum supports the minimum pulse duration of 9.0 fs. The relative flat spectral phase indicates the good compensation of the chirp by the fused silica. The retrieved 9.3-fs pulse duration corresponds to a 1.03 time-bandwidth product (TBP), which is very close to the limit of Fourier transform. This result agrees well with the previous measurement of the similar pulses performed by a FROG setup with a multi-shot configuration[9].

Except for the aforementioned FROG error demonstrated by the retrieved program, the accuracy of the setup depends on the temporal and spectral intervals of every pixel. In our setup, the ambiguity of one pixel of the trace in the camera causes a 1.23-fs uncertainty on pulse duration, i.e., 13% in the results. It becomes even worse in the single cycle regime. The temporal interval can be reduced by using a smaller crossing angle of the two sub-beams or replacing the 4f imaging system with an amplification structure. When the spectrum is over an octave bandwidth, the grating should be substituted by a prism to avoid superposition of the light in the different diffraction orders. Due to the smooth SH efficiency of the thin BBO, this setup is capable to measure the few-cycle pulses with a spectrum ranged from 1.5 to 3 μm with a proper CCD camera and appropriate adjusting the angle between crystal's optical axis and the laser beams.

In conclusion, we report a SHG-FROG setup, which is capable of characterizing few-cycle MIR pulse in single shot. After improving the light splitting method, dispersion caused by transmitting components can be excluded in the measurement. Spectral response correction and specific calibrations are introduced to deal with the extreme bandwidth of the few-cycle pulses in this wavelength range. With the center-wavelength of 1.8 μm, the pulse duration is characterized to be 9.3 fs, which corresponds to about 1.5 optical cycles. This result agree well with the previous measurement with a multi-shot configuration FROG.

This work was supported by the National Natural Science Foundation of China (Nos. 10734080, 60921004, 60908008, and 61078037) and the National Basic Research Program of China (No. 2011CB808101).

References

1. F. Krausz and M. Ivanov, Rev. Mod. Phys. **81,** 163 (2009).
2. P. B. Corkum and F. Krausz, Nat. Phys. **3,** 381 (2007).
3. Z. Zeng, Y. Cheng, X. Song, R. Li, and Z. Xu, Phys. Rev. Lett. **98,** 203901 (2007).
4. Y. Zheng, Z. Zeng, Y. Cheng, R. Li, and Z. Xu, Opt. Lett. **33,** 234 (2008).
5. Y. Zheng, Z. Zeng, P. Zou, L. Zhang, X. Li, P. Liu, R. Li, and Z. Xu, Phys. Rev. Lett. **103,** 043904 (2009).
6. E. Goulielmakis, M. Schultze, M. Hofstetter, V. S. Yakovlev, J. Gagnon, M. Uiberacher, A. L. Aquila, E. M. Gullikson, D. T. Attwood, R. Kienberger, F. Krausz, and U. Kleineberg, Science **320,** 1614 (2008).
7. P. Colosimo, G. Doumy, C. I. Blaga, J. Wheeler, C. Hauri, F. Catoire, J. Tate, R. Chirla, A. M. March, G. G. Paulus, H. G. Muller, P. Agostini, and L. F. DiMauro, Nat. Phys. **4,** 386 (2008).
8. X. Gu, G. Marcus, Y. Deng, T. Metzger, C. Teisset, N. Ishii, T. Fuji, A. Baltuska, R. Butkus, V. Pervak, H. Ishizuki, T. Taira, T. Kobayashi, R. Kienberger, and F. Krausz, Opt. Express **17,** 62 (2009).
9. C. Li, D. Wang, L. Song, J. Liu, P. Liu, C. Xu, Y. Leng, R. Li, and Z. Xu, Opt. Express **19,** 6783 (2011).
10. K. Hong, S. Huang, J. Moses, X. Fu, C. Lai, G. Cirmi, A. Sell, E. Granados, P. Keathley, and F. X. Kätner, Opt. Express **19,** 15538 (2011).
11. C. Iaconis and I. A. Walmsley, IEEE J. Quantum Electron. **35,** 501 (1999).
12. D. J. Kane and R. Trebino, IEEE J. Quantum Electron. **29,** 571 (1993).
13. R. Trebino, *Frequency-Resolved Optical Gating* (Kluwer Academic Publishers, Massachusetts, 2002).
14. A. Baltuska, M. S. Pshenichnikov, and D. Wiersma, Opt. Lett. **23,** 1474 (1998).
15. S. Akturk, M. Kimmel, P. O'Shea, R. Trebino, S. Naumov, E. Sorokin, and I. Sorokina, Opt. Express **11,** 3461 (2003).
16. C. Xu, Y. Leng, C. Zhang, Y. Huang, X. Lu, X. Ge, C. Li, L. Song, and X. Chen, Chinese J. Lasers (in Chinese) **38,** 308004 (2011).
17. S. Akturk, X. Gu, and R. Trebino, in *Proceedings of CLEO Europe* (2005).
18. S. Akturk, C. D'Amico, and A. Mysyrowicz J. Opt. Soc. Am. B **25,** A63 (2008).
19. K. W. Delong, D. N. Fittinghoff, and R. Trebino, IEEE J. Quantum Electron. **32,** 1253 (1996).
20. A. Baltuska, M. S. Pshenichnikov, and D. A. Wiersma, IEEE J. Quantum Electron. **35,** 459 (1999).
21. F. Zhang, Y. Wang, M. Sun, Q. Bi, X. Xie, and Z. Lin, Chin. Opt. Lett. **8,** 217 (2010).
22. D. J. Kane, IEEE J. Set. Top. Quantum Electron. **4,** 278 (1998).